Project no. GOCE-CT-2003-505539

Project acronym: ENSEMBLES

Project title: ENSEMBLE-based Predictions of Climate Changes and their Impacts

Instrument: Integrated Project

Thematic Priority: Global Change and Ecosystems

D2B.20: Preliminary assessment of changes in regional weather and climate over Europe using ENSEMBLES global climate model outputs as they become available

Due date of deliverable: February 2007
Actual submission date: September 2008

Start date of project: 1 September 2004 Duration: 60 Months

Organisation name of lead contractors for this deliverable: FUB and NOA

Revision [1]

Project co-funded by the European Commission within the Sixth Framework Programme (2002-2006)		
Dissemination Level		
PU	Public	x
PP	Restricted to other programme participants (including the Commission Services)	
RE	Restricted to a group specified by the consortium (including the Commission Services)	
CO	Confidential, only for members of the Consortium (including the Commission Services)	

D2B.20: Preliminary assessment of changes in regional weather and climate over Europe using ENSEMBLES global climate model outputs as they become available

While the eventual aim of work in ENSEMBLES WP2B.3 is to produce assessments of changes in regional weather and climate using outputs from the transient RCM scenario simulations being performed by WP2B.1, it was agreed to provide preliminary assessments based on outputs from the ENSEMBLES stream 1 global climate change runs. Unfortunately, delivery of these outputs to the central CERA database was later than anticipated, thus it was eventually decided to use different sources of data, causing a considerable delay in completion of this deliverable. The deliverable consists of two contributions.

The first contribution, from Freie Universität Berlin (FUB), focuses on mid-latitude cyclones and storms. The GCM data required for this analysis was obtained directly from the individual modelling centres – for the A1B scenario runs and 20th century control runs. The results demonstrate the value of a multi-model approach, particularly when the ensemble mean signal is weighted by the quality of each model. This increases the statistical significance of the regional patterns of change. In particular, a robust pattern of an increasing number of extreme cyclones over the Northeast Atlantic and the British Isles is identified.

A short article describing this work has already been published:

Leckebusch, G.C., M. Donat, U.Ulbrich, J.G. Pinto, 2008: Mid-latitude Cyclones and Storms in an Ensemble of European AOGCMs under ACC. *CLIVAR Exchanges*, Vol. 13, No. 3, 3-5. ISSN 1026 - 0471. http://eprints.soton.ac.uk/55670/01/Exch_46_final3.pdf.

A more detailed journal paper about storminess and atmospheric circulation under climate change conditions will be submitted to *International Journal of Climatology* in early autumn 2008:
Donat, MG, Leckebusch GC, Pinto JG, Ulbrich U. European storminess and associated atmospheric circulation in reanalysis data and a multi-model ensemble of GCMs.

A further journal paper should also be finished before the end of 2008. It will be a more extensive consideration of the results presented in the *CLIVAR Exchange* article: Leckebusch, GC, Donat, MG, Ulbrich, U, Pinto, JG. A multi-model ensemble analysis of midlatitudes cyclones and storms under anthropogenic climate change

The second contribution, from National Observatory of Athens (NOA), focuses on climate changes and associated impacts in the Mediterranean resulting from a 2°C global warming – a threshold of particular policy interest and relevance. The work was co-funded by ENSEMBLES and WWF International. Given the delay in delivery of GCM data to CERA, it is based on earlier HadCM3 runs, with bootstrapping used to estimate confidence limits. As well as considering changes in temperature and precipitation, the impacts on agriculture, energy demand, tourism and forest fires are addressed. A detailed paper on this work which will shortly be submitted to *Global and Planetary Change* is included in the Appendix.

Appendix: Draft paper for submission to *Global and Planetary Change*

Climatic changes and associated impacts in the Mediterranean resulting from a 2º C Global Warming

C. Giannakopoulos [1], P.LeSager [1,2], M. Bindi [3], M.Moriondo [3], E. Kostopoulou [1]and CM.Goodess [4]

[1] Institute for Environmental Research and Sustainable Development, National Observatory of Athens, I. Metaxa & V. Pavlou, GR-15236 Palaia Pendeli, Athens, Greece

[2] Atmospheric Chemistry Modelling, Division of Engineering and Applied Science, Harvard University, Cambridge, MA 02138, USA

[3] Department of Agronomy and Land Management University of Florence, 50144 Florence, Italy

[4] Climatic Research Unit, University of East Anglia, Norwich, NR4 7TJ United Kingdom

Corresponding author: Dr. Christos Giannakopoulos
cgiannak@meteo.noa.gr
National Observatory of Athens
Institute for Environmental Research & Sustainable Development
I. Metaxa & V. Pavlou, GR-152 36 Palaia Pendeli, Athens, Greece
Tel: +30-210-8109128
Fax: +30-210-8103236

Abstract

Climatic changes over the Mediterranean basin in 2031-2060, when a 2°C global warming is most likely to occur, are investigated with the HadCM3 global circulation model and their impacts on human activities and natural ecosystem are assessed. Precipitation and surface temperature changes are examined through mean and extreme values analysis, under A2 and B2 future scenario. Confidence in results is obtained via bootstrapping. The basin warming averages about 2°C, and is slightly cooler along the coast and warmer inland. The rate of warming is found to be around 2ºC in spring and winter, while it reaches 4°C in summer. An additional month of summer days is expected, along with 2 to 4 weeks of tropical nights. Increase in heatwave days and decrease in frost nights are expected to be a month inland and two weeks along the Mediterranean rim. In the northern part of the basin the widespread drop in summer rainfall is partially compensated by winter precipitation increase. One to three weeks of additional dry days lead to a dry season lengthened by a week and shifted toward spring in the south of France and inland Algeria, and autumn elsewhere. In central Mediterranean droughts are extended by a month, starting a week earlier and ending three weeks later. The impacts of these climatic changes on human activities such as agriculture, energy, tourism and natural ecosystems (forest fires) are also assessed. Regarding agriculture, crops whose growing cycle occurs mostly in autumn and winter show no changes or even an increase in yield. In contrast, summer crops show a remarkable decrease of yield. This different pattern is attributed to a lengthier drought period during summer and to an increased rainfall in winter and autumn. Regarding forest fire risk, an additional month of risk is expected over a great part of the basin. Energy demand levels are expected to fall significantly during a warmer winter period inland, whereas they seem to substantially increase nearly everywhere during summer. Extremely high summer temperatures in the Mediterranean, coupled with improved climate conditions in northern Europe, may lead to a gradual decrease in summer tourism in the Mediterranean, but an increase in spring and autumn.

Key words: Mediterranean, climate change, extremes, bootstrap, impacts, energy, agriculture, forest fires.

1. Introduction

The global warming predicted by climate models for the 21st century is a threat to most natural systems at every latitude and region. Since its implications are characterised by strong latitudinal variations (IPCC, 2001a; IPCC, 2007), regional studies are proving to be an essential tool for scientists and decision-makers. The present paper investigates climate changes and associated sectoral impacts in the Mediterranean at the time of 2ºC global warming. A global mean temperature change of 2ºC is considered to be a critical level beyond which dangerous climate change occurs. For rising temperatures beyond 2°C, increasing risks of extreme events, distribution of climate impacts or aggregated effects on markets are becoming a growing reason for concern (Smith et al., 2001). In addition, strong positive carbon cycle feedbacks are increasingly likely (Friedlingstein et al., 2003; Jones et al., 2003a; Jones et al., 2003b), which would lead to even more climate change beyond the direct effect of anthropogenic emissions.

While observations limit analyses to local scale (e.g. Fontaine et al. (1999) for the tropical Atlantic), future climate models had to overcome such technical constraints and provide a picture on a wider scale. Regionalization of global models has been performed by three different techniques over the last decade. Statistical downscaling has been applied (Wilby et al., 1998), high-resolution "time-slice" atmospheric general circulation models (Gibelin and Déqué, 2003) and most commonly nested climate models have been developed. However, up to date, they have all focused on the 2070-2100 period as can be seen in the recent EU-funded projects PRUDENCE (Christensen et al., 2002; Räisänen et al., 2003; Giorgi et al., 2004) and MICE (Hanson et al., 2007), or they focus on an indeterminate period when a doubling of CO_2 concentration occurs (Déqué et al., 1998; Jones et al., 1997; Giorgi et al., 1992). Efforts to overcome this temporal limitation are underway through the European FP6 ENSEMBLES project (http://ensembles-eu.metoffice.com).

The closer time of a 2ºC global warming deserves attention, since a general drying has already been detected over most of the Mediterranean (IPCC, 2001b). The region's sensitivity to drought and rising temperature are of prime interest for agriculture, tourism, water resources and policy makers. A global mean temperature change of 2ºC is considered to be a critical level beyond which dangerous climate change occurs. Summer temperatures are likely to increase by more than 2ºC, with a corresponding increase in the frequency of occurrence of severe heatwaves. The 2003 heatwave in Europe (Beniston, 2004; Schär et al., 2004) dramatically illustrates the need to document the extent of climate change for a time period earlier than 2070, as it has been completed by New (2005) for the spectacular changes to occur in the Arctic. This might be beneficial mainly to stakeholders, policy makers and impacts people since they require shorter timescales for their policy planning ahead.

Since the time of a 2ºC global warming is expected between 2026 and 2060 (section 2), at the time of the experimental runs for this paper, only General Circulation Models (GCMs) were available to assess the climatic characteristics in the Mediterranean during this period. Although GCMs present a range of sensitivity to greenhouse gas and aerosol forcing, which in turn depends on emission scenarios for future estimates, only data from one model, the HadCM3, have been used in the present study. As discussed in sections 2 and 5, the results are representative of the currently available global climate models for the considered time period. Climatic changes are determined through comparison between control (1961-1990) and future

(2031-2060) years. Surface temperatures (section 3) and precipitation patterns (section 4) are examined. Means and extremes are used to describe future changes. Seasonal and yearly parameters are considered. The confidence in the estimated changes for each parameter is important and determined with the bootstrap method.

2. Method and the 2ºC global warming

2.1. Model choice and the 2ºC warming

New (2005) carefully addresses the time of 2ºC global warming predicted by GCMs. Considering 21 climate change simulations from six GCMs and four IPCC emissions forcing scenarios, series of global mean temperature-anomalies, defined as difference with pre-industrial value, have been calculated. The time of 2ºC global warming found by New (2005) is between 2026 and 2060, depending on the sensitivity of the model to greenhouse gas forcing and to future scenarios. The various series are reproduced in Fig. 1. Model comparison studies have shown that results from different models for the 2026-2060 period agree with one another fairly well, while most of the divergence takes place in the latter part of the century (2070-2100) (IPCC, 2001b). The same conclusion is drawn from Fig. 1, particularly if the outlier series cgcm1/2 IS92aGG (scenario with greenhouse gas only) is disregarded. The range of simulation results starts to really spread after 2060. To study the 2026-2060 period, considering 20 simulations, or just one with an average response, to forcing scenarios will give similar results. The advantage of using one model resides in the knowledge of its weaknesses and shortcomings, which can prove important in interpreting results.

In the present study, output from the HadCM3 model (Gordon et al., 2000; Pope et al., 2000) driven by SRES A2 and SRES B2 scenarios are used. The model couples an atmospheric GCM to an ocean GCM. Unlike earlier atmosphere-ocean GCMs, flux adjustment (i.e., additional artificial heat and freshwater fluxes at the ocean surface) is not required to produce a simulation. The high ocean resolution of HadCM3 is a key factor in this improvement. The atmospheric component of HadCM3 has 19 levels with a horizontal resolution of 2.5° of latitude by 3.75° of longitude, which produces a global grid of 96 x 73 grid cells. This is equivalent to a surface resolution of about 417 km x 278 km at the Equator, reducing to 295 km x 278 km at 45° of latitude (comparable to a spectral resolution of T42). Hence, the model geography is much simpler than the real-world geography. As an example, only two grid cells cover Greece, one land (northern Greece) and one sea (southern Greece) grid cell. The oceanic component of HadCM3 has 20 levels with a horizontal resolution of 1.25 x 1.25°. At this resolution it is possible to represent important details in oceanic current structures. Mediterranean water is partially mixed with Atlantic water across the Strait of Gibraltar as a simple representation of water mass exchange, since the channel is not resolved in the model.

HadCM3 has been run for over a thousand years, showing little drift in its surface climate. The control run is basically the GCM being run for 240 years at 1961-1990 atmospheric concentrations. Any variation in the control run stems from natural variability. The last 30 years of the control run, 1961-1990, are used here as reference for comparison with future predictions. The control run is unforced and thus common to any scenario that may apply after 1990. Here we considered the A2 and B2 emissions scenarios. These depend on several drivers such as population growth, economic and technological development, natural resources etc (Nakicenovic et al., 2000). With a population of 15 billion by 2100, the A2 world undergoes a greater rate

of warming than the B2 world with its medium 10.4 billion population projection and its focus on local solutions to economic, social and environmental sustainability.

Indication of HadCM3 average response to forcing scenarios is provided by its transient climate response (TCR). The TCR is commonly used to compare model responses to a same standardised forcing. The TCR of HadCM3 is 2°C, which occupies an average position within the range of TCRs (1.4°C – 3.1°C) of the 19 GCMs assessed in the IPCC Third Assessment Report (*IPCC*, 2001b). Characteristics for both scenarios are shown in Fig. 1. A pair of black squares (circles) indicates the temperature anomaly according to HadCM3 under A2 (B2) scenario in 2026 and 2060. The HadCM3 clearly exhibits an average response for A2 and a conservative one for B2, with respective to the time of 2°C global warming of 2049 and 2060. Regarding changes in climatic means and extreme values, results from both scenarios are so similar for the period considered here that they are collected together to improve their confidence levels (see section 3).

2.2. Method description

Based on daily model outputs, each annual parameter (an extreme, a mean or accumulated value) is computed and averaged over future (2031-2060) and control (1961-1990) years. Note that the 2026-2060 period of section 2 is reduced to 2031-2060, because the same number of years is required to bootstrap the differences. The difference between both averages is examined using a confidence estimate. With respect to the difference, the control period is subtracted from the future, except in one instance clearly noted below. Thus positive values indicate an increase in the future. The confidence in estimated changes is obtained by bootstrapping (Mudelsee and Alkio, 2007) the differences between the two periods. The method resamples the annual difference parameter 1000 times with replacement and calculates the mean of each sample. The 95-percentile confidence limits are computed based on the resulting series. In the resampling process each sample consists of 30 values.

As A2 and B2 deliver similar results, in terms of regional spatial detail, we pieced both simulation outputs together and repeat the procedure to get A2/B2 average results. In the process, the sample population is doubled to 60, and confidence limits are higher. In the present study, these A2/B2 results are shown interpolated by a minimum curvature surface procedure onto a 2.5°x0.7° longitude-latitude grid. The same method (difference, bootstrapping, and A2/B2 averages) is applied to all studies that follow.

3. Temperature changes

3.1. Annual and seasonal averages

The Mediterranean basin will experience an average 2ºC warming at the same time as the average globe. Because of the latitudinal variation in the amount of warming at the time of a 2ºC global warming, we first look at changes in annual mean temperatures. The left column of Fig. 2 shows maps of changes in annual mean of daily maximum (Tmax), mean (Tmean) and minimum (Tmin) temperatures. The confidence range in the right column is the difference between the upper and lower confidence limits. It is mainly a practical way to present these limits into one plot. Dividing the confidence range by two gives the value to add or subtract from the mean difference in the left column to get the limits. For example, we are 95% confident that the rise in Tmean along the Mediterranean rim will be between 1.8 and 2.2ºC (2°C ± 0.2ºC). This is a 10% uncertainty in the prediction. Due to the thermal

inertia of the Mediterranean Sea, the daily mean temperature rise (Fig. 2b) is between 1-2ºC (± 0.15) along the coast, and 2-3ºC inland (± 0.25). It is slightly larger in daytime (Fig. 2a), exceeding +3ºC in the Balkans. In the south of France and the Iberian Peninsula, the rise is slightly lower at night-time (Fig. 2c).

Seasonal changes, shown in Fig. 3 for the daily mean, are more pronounced, and have more uncertainty. The rise occurs mainly in summer (Jun/Jul/Aug), when it reaches 4ºC inland on average. It rises above this value in the Balkans, Turkey, north Italy, and Spain, with a confidence of about ± 0.75 ºC (18%). Autumn (Sep/Oct/Nov) has the second largest warming in absolute terms: mean temperatures rise above 2ºC (± 18%). Winter (Dec/Jan/Feb) is likely to be warmer by 1-2 ºC with an uncertainty of 25% (± 0.25-0.5 ºC). Spring (Mar/Apr/May) has a very similar pattern, but with slightly more warming in the Asian side. Since Tmax and Tmin present the same seasonal variations as Tmean, they are not shown here. However, a smaller summer increase at night (Tmin) and a larger daytime increase (Tmax), both by about 1ºC, are found inland but not along the coast.

3.2. Temperature Extremes

Better insight into the future Mediterranean climate can be gathered from extreme values of climatic variables. We have chosen indices of extremes with fixed thresholds appropriate for the Mediterranean climate as fixed threshold values are easier for impacts people to understand and use. The following annual indices of temperature extremes have been calculated:

- Number of summer days (Fig. 4a), defined by Tmax > 25 ºC
- Number of hot days (Fig. 4b), defined by Tmax > 30 ºC
- Number of heatwave days (Fig. 4c), defined by Tmax > 35 ºC
- Number of tropical nights (Fig. 4d), defined by Tmin > 20 ºC
- Number of frost nights (Fig. 4e), defined by Tmin < 0 ºC

Note that units are in weeks, and the convention used in this paper is exceptionally broken in Fig. 4e, where the difference between both periods is obtained by subtracting the future period from the common one. In other words, Fig. 4e features an estimated decrease, while other figures show increase estimates. The largest increases are found in summer days (up to 8 weeks in Crete) and tropical nights (up to 10 weeks in the easternmost Mediterranean). These indices (Figs.4a and 4d) are moderate extremes. The Mediterranean Sea does not temper their increase, as opposed to the more extreme indices (Figs.4b, 4c, and 4e).

3.2.1. Moderate temperature extremes

Overall, about one additional month of summer days is expected (Figure 4a). Summer days increase more in the milder northern part of the basin, up to 6 (± 1) weeks inland, and less in the Maghreb and the easternmost part of the region. An exceptionally large summer increase is projected to affect the south of Greece and in less measure the south of Italy, but it should be borne in mind that these areas are represented as sea in the HadCM3 model. The longer summers are accompanied by additional tropical nights (Fig. 4d), again particularly in the central part of the basin. However, the north/south dichotomy is inverted: the augmentation mainly affects the southern part, while lots of nights in the northern part remain below the 20ºC threshold, despite the night-time warming (Fig. 2d). To summarise, we have defined three broad regions:

- the northern withl add more than a month of summer and half-month of tropical nights,

- the southern with about one month more of summer and more than a month of tropical nights, and
- the central (represented as sea in the model) with a large increase of both extreme indices.

Note that the easternmost area (Lebanon, Israel fits more in the second than the third region and displays large uncertainties.

3.2.2. High temperature extremes

Increases in the number of hot (Fig. 4b) and heatwave (Fig. 4c) days, as well as decrease in the number of frost nights (Fig. 4e), have a similar spatial pattern with slightly different magnitudes depending on the location. Increases range from 2 weeks (± 0.5) along the Mediterranean rim to about a month (± 0.5-1 week) inland. Owing to its proximity to the Atlantic Ocean, only one land grid cell runs across the Pyrenean chain, the south of France appears less sensitive to high extreme changes. On the contrary, three model land grid cells separate the ocean from the sea across the Iberian Peninsula, where the ocean proximity is not felt in extreme indices. Note also that the increase in the north Aegean Sea relates to a land cell in the model, and should not be used to draw conclusions for the Aegean Sea itself.

4. Precipitation

4.1. Annual and seasonal totals rainfall

The second part of the study focuses on the precipitation regime. As shown in Fig. 5e (centre), annual total rainfalls mainly decrease. The spatial? variation (Fig. 5e-left) is relatively small. It is less than 10% in the major part of the Basin, and between 10 and 20% in the already drier southern part. Uncertainties (Fig. 5e-right) are a lot larger than for temperature changes. They are above ±50% of the expected change everywhere (Pyrenees and Southern Turkey are the only exception with an uncertainty between 25 and 50%). They are roughly in the 75-150% range where the future changes are significant (~ >20mm). These large uncertainties might stem from large intra- and interannual variabilities. The intraannual variability can be perceived in seasonal variations pictured in Fig. 5a-d and discussed below. The interannual variability of precipitation is well known (Bolle, 2003; Lionello et al., 2006) and reproduced in the simulations.

The difference between emission scenarios does not significantly contribute to the uncertainties. The largest differences between A2 and B2 are found in Portugal and over the Adriatic Sea. The B2 scenario predicts some increase (occurring mainly in winter), while A2 predicts a decrease in precipitation. However, both cases include huge uncertainties in these areas (above ±200%). The uncertainty associated with Portugal in Fig. 5e (right) is only due to intra- and interannual variability. In other words, the differences between the two scenarios are not statistically significant when other uncertainties are taken into account. Finally, better confidence is gained by piecing together the two simulation results.

The picture of a globally drier Mediterranean Basin conceals seasonal variability as shown in Fig. 5a-d. The main features are the winter and summer changes in the north of the Basin. The latter becomes wetter in winter (about +10%), but this is largely compensated by a drier summer (–30%). Autumn (Fig. 5d) is the season with the fewer changes. On the other hand, the southern Mediterranean is projected to endure an almost evenly distributed small decrease in precipitation all year long. Note that the drier north is the most reliable expectation with less than

±50% uncertainty. Autumn reveals the largest uncertainty that rises above 200% in most of the area, but the changes are small in absolute terms. In summary, a globally 10% drier Mediterranean region is expected. The precipitation decrease will be spread over the whole year in the south and will be the result of a summer decrease partially balanced by an increase in winter in the northern part (Christensen and Christensen, 2007; Déqué et al., 2007).

4.2. Extremes

Further insight is gathered in investigating the number of dry days and spells, and the annual maximum running total rainfall over three days. We have chosen the three-day total in order to catch total rain amount accumulated over this short time period that may have the potential to cause localised flooding. Days are qualified as dry if daily precipitation (RR) amounts to less than 0.5 mm, a typical threshold value in modelling studies (Hanson et al., 2007). The change in the number of these days is shown in Fig. 6a in week unit. The 2ºC global warming is characterised by 1-3 weeks (± 5 days) of additional dry days. The spatial pattern follows the temperature increase with smaller changes (approx. 1 week) in the already dry southeast basin and along the coast, and larger ones inland. The Iberian Peninsula, the Balkans, Turkey and the south of France feature the largest increase (above 3 weeks).

Similar results are obtained if the daily precipitation threshold is raised to 1 mm. The number of wet days (RR>10mm) and very wet days (RR>20mm) feature ± 3 days of change for the former and none for the latter. We conclude that the increase of dry days is concomitant to a decrease of rainy days (not shown) within the 1-10mm RR range. Not surprisingly, the longer wet spells show little change in their length. However, the longest droughts (Fig. 6b) lengthen by about a week. Although the uncertainties are large, it is worth noting that in the centre of the Mediterranean Sea the drought season will become longer by approximately one month, which is larger than the increase in number of dry days. This conveys a tendency for aggregation around summer, while other regions see their additional dry days being more scattered throughout the year. This tendency is confirmed by the fact that the spatial pattern of droughts is similar to the pattern of the increase in summer days (Fig. 4a).

Although they are not strictly extreme indices, the average shifts of start (Fig. 7a) and end (Fig. 7b) of the longest drought are worth examining, because of their interest for agriculture and the tourism industry. In Fig. 7, a positive value means a shift toward the year-end. The general tendency is a small shift (slightly larger under B2 than A2 scenario) toward autumn, with the exception of the south of France and inland Algeria where the longest droughts start and end two week earlier on average. The uncertainties are still large, except in the centre of the Mediterranean basin, where the longest droughts will start a week earlier and end 3 weeks later, in accord with the one-month lengthening (Fig. 6b). Both estimates have a ±1 week uncertainty. The annual maximum running total rainfall over three days is an extreme index and shown in Fig. 8. The rain intensification seen on the northern half is a direct consequence of precipitation increase during winter (Fig. 5a). On the contrary, the steady small precipitation decrease all year long in the southern half leads to lower highest accumulated rainfall. The uncertainties range between ±100%.

5. Impact analysis

5.1. Agriculture

5.1.1. Simulation model and crop selection

CROPSYST (Cropping Systems Simulation Model) was selected as simulation model for this work (Stockle et al, 2003) and HadCM3 data of hotspot cells (Tmin, Tmax, rainfall and global radiation) were used as input data. This is a multi-year, multi-crop, daily time step crop growth simulation model, which simulates the soil water budget, the soil-plant nitrogen budget, crop canopy and root growth, crop phenology, dry matter production, yield, residue production and decomposition, and erosion. The model allows the user to specify management parameters such as sowing date, cultivar genetic coefficients, soil profile properties, fertilizer and irrigation management, tillage and atmospheric CO_2 concentration.

The simulation of crop phenology is mainly based on the thermal time required to reach specific development stages. Thermal time is calculated as growing degree days (GDD, °C day^{-1}) accumulated throughout the growing season (starting from planting until harvest). The capability of the model to simulate crop yields has been evaluated in numerous field studies conducted in the Mediterranean, United States and Australia (Stockle et al., 2003). In general, the agreement between simulated and measured yields is good. When properly calibrated and applied, CROPSYST has proved to be a suitable tool for simulating cropping systems. On the basis of results obtained in the previous section, 13 grid cells (hotspots) of the HadCM3 were selected for agriculture impact assessment (Table 1). More specifically these grid cells were selected both to provide an homogenous cover of the domain and to study the areas where changes in precipitation and temperature patterns are expected to be substantial, according to the model simulations.

With respect to each hotspot, five types of agricultural crops, having different characteristics based on i) photosynthesis pattern (C3 and C4 crops), ii) growing period (winter and summer seasons), iii) food composition (protein, e.g. legumes and carbohydrates, e.g. tuber crops), were selected on the basis of their relative importance (Table 1), as have been reported in the FAOSTAT database (http://faostat.fao.org/). Crop cultivated areas were used as proxy indicator to assess the relative importance of each crop in the countries where the hotspots grid cells are included. No account has been taken of the introduction of new crops which may become suitable in these regions. Accordingly CROPSYST model was run, for crops listed in table 1, using 2 different configurations: 1) default version, to assess model performance using the default crop growth parameter; 2) calibrated version, where crop growth parameters were modified in order to obtain the lower differences between observed and simulated yield.

The calibrated version of CROPSYST was then applied both to assess climate change impact on crop yield in future scenarios A2 and B2 and to evaluate the application of adaptation strategies to face possible yield losses. Regarding the present climate the simulation runs were done setting the atmospheric concentration of CO_2 at 350 ppm while two different simulations were performed for future climate scenarios where increased CO_2 concentration was not included (1, $[CO_2]$=350 ppm) and included (2, $[CO_2]$=470 ppm and $[CO_2]$=520 ppm for B2 and A2 scenarios respectively). Potential crop growth was specified to increase in a doubling CO_2 environment by 20% for C3 crops (wheat, barley, sunflower, bean, potato, soybean) and 10% for C4 crop (Maize) and the same response for crops within each of the two classes was assumed. In all the simulation runs the C4 summer crops and tuber crops

were considered as “irrigated crops”, whereas the rest of the crops were considered as “rain-fed crops”. Nitrogen was considered not limiting for all the crops.

5.1.2. Results

The calibrated version of CROPSYST for the present climate captured correctly the spatial pattern of yield level across the Mediterranean basin (data not shown). Results showed a clear pattern in rain-fed crops that is strongly correlated to the precipitation regimes of the different grid cells. Lower crop yields were observed in Northern Africa regions, which are expected to have lower water availability, whereas for the irrigated crops, the differences in crop yields among the grid cells were less evident being mainly driven by the temperature regimes.

To provide a quantitative estimate of the uncertainties related to the capacity of CROPSYST to simulate crop yields, prediction error was calculated for each crop type in each hotspot and final results were summarised for four main regions in the Mediterranean basin: North-West region (N-W) including Portugal, Spain, France and Italy, North East region (N-E) including Serbia, Greece and Turkey, South East region (S-E) including Jordan, Egypt and Libya and South West region (S-W) including Tunisia, Algeria and Morocco (Table 2). Prediction error was expressed as Mean absolute error (MAE) that is the average of the difference between modelled and observed value in all test cases. The climate conditions of the grid cells cannot completely represent the average condition over a nation, and the statistical data also include sources of variability (e.g. technological trend, pest and disease stresses, etc.) that cannot be reproduced by the model. The results showed that CROPSYST results match quite closely with the statistical data collected by FAO, with MAEs ranging from less than 1% to under 14%. The MAEs can also be used as a measure of the uncertainties of crop yield estimates due to the bias between observed and simulated yields. The total uncertainty is likely to be larger due to the uncertainties cascaded from the emission scenarios and the global climate model.

The results of the CROPSYST simulation runs, without including the effect of increased CO_2, for present and future climate scenario, on the basis of the different crop types, can be summarised as follows (Fig. 9): C4 summer crops show an almost systematic reduction of yields with the exception of a few grid cells located in the EU-Mediterranean countries (e.g. Italy, France, Spain and Portugal). Legumes show a general reduction of yields in all the grid cells with the exception of that on Spain, where, however, the increase was very small. C3 summer crops showed a general reduction of yields in all the grid cells with the exception of that on Spain, where, however, the increase is very small. Tuber crops show a general reduction of yields in all the grid cells with the exception of those on Jordan and Spain. Cereals show a general reduction of yields, even if in a few grid cells the yields increase (Turkey, Greece and Spain; Fig. 9e). In general, a substantial reduction is revealed for all the crop types in all ‘hot spots’ grids. This is due to the increases in temperature and reduction in precipitation predicted for both future climate scenarios (A2 and B2), which determine a general reduction in growing period duration and in water available for crop growth, respectively. Decreases are larger for non-irrigated crops in summer.

In contrast when the effect of increased CO_2 is not included in the CROPSYST simulation runs, the results of the different crops types for present and future climate scenario, can be summarized as follows (Fig. 10): C4 summer crops show a prevalent reduction in yields in the grid cells located in the African and Asian Mediterranean countries (e.g. Morocco, Tunisia, Jordan, etc.); whereas on the

European grid cells yields show a consistent increase. Legumes show a general reduction of yields in all the grid cells with the exception of those on Spain, Turkey and Greece. C3 summer crops show a general reduction of yields in the grid cells located on Northern and South-western shores of the Mediterranean basin; whereas in the grid cells located on the Southern or Eastern shores, yields are substantially unchanged. Tuber crops show an inconsistent response among selected grid cells, with a general reduction of yields in those on the African shores of the basin, and prevalent increase in the rest. Cereals show a prevalent increase in yields. In summary, the effect of climate change on agriculture is likely to be more severe in southern Mediterranean areas than the northern temperate areas. In the warmer southern Mediterranean, increases in CO_2 help to reduce the loss in yield arising from a warmer and drier climate, but are not able to completely recover the losses. In the cooler northeastern Mediterranean, the CO_2 increases result in little net effect on most crops, provided that the increase in water demands, especially for irrigated crops, can be met.

Introduction of adaptation strategies indicates different options to reduce the impact of global change according to crop type. Anticipation of the sowing date associated to the shortening of growing season may allow crops to escape the higher temperature and water stress simulated by HadCM3 in summer for both A2 and B2 scenarios, and this results in a relative increase of final yield. The use of longer growing cycle cultivars proves to be a worthy adaptation strategy too, in future scenarios where higher temperatures trigger increase of development rate. Both options, however, would require additional water for irrigation. In particular, the effective use of long-cycle cultivars can demand 25 – 40 % more water, which may be not available or not cost effective in the future.

5.2. Energy demand

Energy demand is linked to climatic conditions (Giannakopoulos and Psiloglou, 2006) and the relationship of energy demand and temperature is non-linear. The variability of ambient air temperature is closely linked to energy consumption, whose maximum values correlate with the extreme values of air temperature (maximum or minimum). In the Mediterranean region, during January, the maximum values of energy consumption are related to the appearance of the lowest temperatures. During the transient season of March-April, energy consumption levels are kept nearly constant until about May, while air temperatures are constantly rising. From mid-May onwards, and throughout the summer period, any increase in air temperature corresponds to an increase in energy consumption mainly due to the extensive use of air conditioning systems. An exception is found for August when most local people tend to take their summer holidays, and hence the demand for air conditioning is reduced especially in large Mediterranean cities. Another transient period exists in the months of September and October where energy demand and consumption are kept at constant levels. This transient period is followed by a period of continually increasing energy demand with a peak before the Christmas festive period. Therefore, it is anticipated that warmer climate conditions will lead to decreased demand in winter, while increased demand should be typical during summer time (Valor et al., 2001; Giannakopoulos and Psiloglou, 2006). Moreover, the effect of higher temperatures in summer is likely to be considerably larger on peak energy demand than on net demand, suggesting that there will be a need to install additional generating capacity over and above that needed to cater for underlying economic growth.

Since the energy-temperature relationship is non-linear and has two branches, it would be more convenient to separate these two branches. The easiest way to achieve this is to use the idea of Degree-Day, which is defined as the difference of mean daily temperature from a base temperature. Base temperature should be the temperature where energy consumption is at its minimum. If this temperature is chosen, then the degree-day index is positive in the summer branch and negative in the winter branch. Instead of having both positive and negative values for this index, the definition of two indices is used: heating (HDD) and cooling degree days (CDD). For the calculation of the HDD and CDD indices, the following equations were used:

$$HDD = \max (T^* - T, 0) \quad \text{(Eq. 1)}$$
$$CDD = \max (T - T^{**}, 0) \quad \text{(Eq. 2)}$$

where T^* and T^{**} are the base temperatures for HDD and CDD respectively, which can be either the same or different and T is the mean daily temperature calculated from the daily data of HadCM3 for both the reference and the future periods.

HDD (CDD) is a measure of the severity of winter (summer) conditions in terms of the outdoor dry-bulb air temperature, an indication of the sensible heating (cooling) requirements for the particular location. Kadioğlu et al. (2001) used different base levels of 15^{o}C and 24^{o}C for the calculations of HDD and CDD respectively in Turkey.. In our study we use 15^{o}C for the calculation of HDDs and 25^{o}C for the calculation of CDDs. We identify the changes in energy demand levels by showing differences in the cumulative numbers of CDDs and HDDs between the reference and the future period.

5.2.1 Cooling energy requirements

In general, more energy will be required for cooling. Over the year the increase in CDD is be large in south Mediterranean (from Gibraltar to Lebanon), i.e., in the Middle East and the North African part of Mediterranean region (Fig. 11). In northern side, the main increase is in the south Iberian Peninsula, north-Italy-Balkans-Greece, and south Turkey. The seasonal changes in CDDs have also been examined (not shown). As expected the main contribution is from summer, with no increase in winter, and a very small increase in autumn and spring. The only regions to escape any significant increases in cooling energy demand are: south Italy (including Sicily and Sardinia), south of France, Cyprus, northern part of Turkey (in the proximity of Black Sea), and the north-western tip of Spain. Fig. 12 presents another view on the increase of energy demand by showing the number of days when this demand is needed to cool more than 5^{o}C. In the southern part of the Mediterranean Sea, from the south of the Iberian Peninsula and North African coast to Syria, an additional month of heavy cooling is required. The 2 to 3 week increase in the north Aegean area is also worth mentioning.

5.2.2. Heating energy requirements

In general, less energy is required for heating. Fig. 13 shows the spatial distribution of the general decrease in HDDs. It can be emphasised that:

- The largest decrease occurs in the northern side of the region, from Turkey to north Italy.
- Spain and France see a smaller but still noteworthy decrease,

- The south-eastern Mediterranean exhibits the lowest decrease, mainly because it is already a warmer region.

Note also the cooling effect of the sea along the coasts. Unlike the CDD rise, the HDD decrease is spread over the year (not shown), although this probably depends to some extent on the choice of base temperature. Naturally, winter is the season that will require much less heating. The largest changes occur along and above the axis North-Italy-Balkans-Greece-Turkey. As shown in Fig. 14, the decrease in the number of days that require energy to warm more than 5^{o}C (HDD>5) varies from about 2 weeks along the coast to a month inland.

5.3. Forest Fire Risk

5.3.1 Fire Weather Index (FWI)

One of the potential detrimental impacts of anthropogenic climate change is increased wildfire occurrence. Mediterranean Europe, in particular, has been identified as likely to suffer potentially increased fire risk (Pinol et al., 1998; Moriondo et al., 2006). The contribution of meteorological factors to fire risk is simulated using various non-dimensional indices of fire risk. Viegas et al. (1999) validated a number of fire indices in the Mediterranean against observed fire occurrence, and the Canadian Fire Weather Index (FWI, van Wagner, 1987) was among the best performers. Viegas et al. (2001) demonstrated that in summer, the slow response of live fine fuel moisture content to meteorological conditions is well described by the Drought Code sub-component of the FWI system. In addition, FWI is one of the most widely used indices of fire risk. Therefore, output from climate model simulations of the coming decades was used to the FWI model to examine potential changes in Mediterranean fire.

The Canadian Fire Weather Index system is described in detail in van Wagner (1987). Briefly, it consists of six components that account for the effects of fuel moisture and wind on fire behaviour. These include numeric ratings of the moisture content of litter and other fine fuels, the average moisture content of loosely compacted organic layers of moderate depth, and the average moisture content of deep, compact organic layers. The remaining components are fire behaviour indices, which represent the rate of fire spread, the fuel available for combustion, and the frontal fire intensity; their values rise as the fire danger increases. Fire risk is low for FWI<15, and increases more rapidly with FWI>15 (Good et al., 2008). A threshold of FWI>30 was selected as a measure of increased fire risk.

5.3.2 FWI results

The monthly changes of average FWI from May till October between the future and the control period have been examined (not shown). We note that:

- The increase is higher during the summer, with the maximum increase in August in the North Mediterranean inland.
- Balkans, Maghreb, north Adriatic, central Spain, and Turkey seem to be the most vulnerable regions.
- South of France is as strongly affected as Spain, but only in August and September.
- The south-eastern Mediterranean (from Lebanon to Libya) sees no particular increase or decrease.

- The same seems to hold for the islands of Crete, Sardinia, Sicily (southernmost Italy too), Peloponnese, and Cyprus. Cyprus may even see a small decrease every month.
- The results are very similar under scenario B2 (not shown).

Fig. 15 shows the increase in the number of days with fire risk (top) and extreme fire risk (bottom).

According to this figure, the increase in the mean FWI is translated into:

- 2 to 6 additional weeks of fire risk everywhere, except south Italy and Cyprus and the south-eastern Mediterranean.
- The maximum increase is again inland (Spain, Maghreb, Balkans, North Italy, and Central Turkey), where at least an additional month with risk of fire has to be expected.
- A significant proportion of this increase in fire risk is actually extreme fire risk (FWI>30).
- South of France, Crete, and the coastal area of the rest of Mediterranean Region: significant increase in the number of days with fire risk (1-4 weeks), but not in the number of extreme fire risk.

5.4. Impacts on Tourism

As some measure of the economic importance of summer tourism to the Mediterranean, 147 million international tourists visited the Mediterranean in 2003 (this is 22% of the international tourism market) and generated US$113 billion for the region (WMO, 2004a,b). A large percentage (70%) of these tourists visited just two countries, Italy and Spain. It is very difficult to model the potential response of tourists to climate change. However, by discussions with experts at the MICE regional workshop entitled "Impacts of climate extreme events on Mediterranean tourism and beach holidays", (which took place in June 2004 in Crete), it was possible to identify some of the impacts climate change may have on the tourism industry (Table 3).

Rising temperatures over the Mediterranean region in 2031-2060 will certainly affect the thermal comfort of tourists and their ability to acclimatise to a region prone to high temperatures and heatwaves. Rainfall is also projected to decrease, leading in turn to shortages in the public water supply and more widespread desertification, which may affect the aesthetics of the region. Water shortages due to extended droughts will also affect tourism flows especially in the SE Mediterranean since the water use has a strong seasonal cycle. The maximum demand coincides with the minimum availability. Perry (2001) reports that a tourist in Spain uses four times as much water as a Spanish city dweller, so tourists are not water conscious. He also states that in Crete water shortages could be experienced in 5 years out of 6 by 2010. As noted earlier in this paper, the combined effect of decreased rainfall and increased temperatures will lead to a greater frequency of forest fires. Intense rainfall events in winter may increase especially in the northern part of the region, leading to greater erosion rates and a higher risk of flooding. Greater heat is also likely to repel at the same time the important old age population and the residents of Mediterranean regions, in France, Italy or Spain. Thus mountainous regions could become appreciated for their relative coolness and the shade of their forests (Ceron and Dubois, 2000).

It is not, however, just the change in climate over the Mediterranean that will impact on the region's tourism. Improvements in the climate of the source regions of the tourists visiting the Mediterranean will also affect the popularity of the area. Warmer, drier and more reliable summers in Northern Europe will encourage tourists

to take domestic holidays and will even encourage those in the Mediterranean region to holiday further north, away from the high temperatures and water deficits likely in the south during summer. It is also likely that the Mediterranean holiday season will split into two seasons, in the spring and the autumn, when climate conditions will be more comfortable (Perry, 2005; IPCC, 2007).

In conclusion:

- Warmer northern European summers encourage an increase in domestic holidays.
- In a warmer future, there is an increased likelihood of people from the Mediterranean holidaying in the north.
- More frequent and more intense heatwaves and drought are likely to discourage Mediterranean summer holidays.
- There is likely to be a shift in the Mediterranean holiday season to spring and autumn.

6. Conclusions and discussion

The climate change in the Mediterranean at the time of a 2ºC global warming has been examined. The basin will experience an average 2ºC warming at the same time as the average globe. The spatial pattern is characterised by a slightly lower warming along the coast, and slightly larger inland. This fine scale structure is also found with regional models by Giorgi et al. (2004) and Räisänen et al. (2004), both with greater magnitude since their studies cover the latter decades in the century (2070-2100).

Strong seasonal dependence is apparent with an average warming up to 4ºC in summer, above 2ºC in autumn and below 2ºC in spring and winter. Studies of European impacts of a CO_2 concentration doubling (Giorgi et al., 1992, Déqué et al., 1998) give similar values. The feature of maximum summer warming in the centres of the Balkans and the Iberian Peninsula appears to be common in climate change simulations (Giorgi et al., 2004; Déqué et al., 1998). The lower in winter and larger in summer temperature anomaly is also a robust finding as documented in IPCC reports (IPCC, 2001b, 2007). It is common to GCMs and RCMs as shown for example by Gibelin and Déqué (2002) for the B2 scenario in 2070-2100 (Hanson et al., 2007; Christensen and Christensen, 2007; Déqué et al., 2007).

The analysis of annual indices of temperature extremes divided the study region in three sub-regions. The northern basin has an additional month of summer and half-month of additional tropical nights. The southern basin has an additional month of both summer and tropical nights. An exceptionally large increase of summer (more than 2 months) is expected in the basin centre, which is modelled exclusively as sea. These increases only have inland repercussions on highest extremes. The number of heatwave days (frost nights) increases (decreases) by up to a month inland, but by only two weeks along the coast.

Simulated precipitation regimes depict a globally drier Mediterranean in 2030-2060, with a 10-20% drop in annual rainfall. The drop results from a large summer decrease partially balanced by winter increase in the northern part of the region. The precipitation changes in the intermediate seasons are less pronounced than in winter and summer. In the southern part, the seasonal dependence is smaller. Following the winter precipitation increase in the northern basin, the annual maximum running total rainfall over three days shows intensification. Increase in precipitation intensity has been reported in other regions, even in regions where the mean precipitation decreases (Giorgi et al., 2004). The widespread summer negative trend is a common feature of

regional climate change simulations (e.g. Jones et al., 1997; Giorgi et al., 2004; Räisänen et al., 2004). However, precipitation changes present large uncertainties, and differences with other simulations are expected. For example, Déqué et al. (1998) report large precipitation increases (+30%) in the south in winter at time of a CO_2 concentration doubling, although their simulation reflects conditions closer to those of a 2ºC global warming than the majority of 2070-2100 studies.

Nevertheless, our conclusion of a drier Mediterranean in 2031-2060 translates into about one week of additional dry days along the coast and in the already dry southeast basin. Inland of the northern basin, up to and over 3 weeks of additional dry days are expected. No supplementary wet or very wet days are expected. Consequently, longest droughts get longer by about a week in general and exceptionally by a month in the centre of the Mediterranean basin. The dry season tends to shift toward autumn, with the exception of the south of France and inland of Algeria where it starts and ends two weeks earlier on average.

The dry season shift and lengthening call for more accurate seasonal analysis through a study on their monthly variations. To get a truly additional insight into climatic changes, regional models that account for the topography at regional scales, and particularly coastline features, are required. This is of great importance for precipitation patterns that already show high regional variability in the contemporaneous climate and particularly in areas with contrasted topography near coastland (Türkeş, 1998; Romero et al., 1999; Xoplaki et al., 2000; Kostopoulou and Jones, 2005). Finally, weighted multi-model ensembles of simulations would provide a more robust assessment of climatic changes and the ENSEMBLES EU-project will allow this type of study to be repeated using Regional Climate Models.

Our study showed that the increases in temperature and reduction in precipitation predicted for both future climate scenarios (A2 and B2) lead to a substantial reduction of yields for all the crop types in all the 'hot spots' grid cells, through the reduction of the length of the growing period and the water available for crop growth. Reductions in yields are more severe in the warmer southern Mediterranean than in the cooler northern Mediterranean, even when the fertilizing effect of increased CO_2 is taken into account. The southern Mediterranean is likely to experience an overall reduction of yields due to climate change. In some locations in the northern Mediterranean, the effects of climate change and its associated increase in CO_2 may have little or small positive impacts on yields, given that additional water demands can be met.

Strategies such as early sowing dates or cultivar with slower development rates may be considered as advisable options to reduce some of the reductions in crop yield determined by the changes in climate conditions. However, such options could require up to 40% more water for irrigation, which may or may not be available in the future. Moreover, according to recent studies on the effects of tropospheric pollutants such as ozone on crop yields, there is reason to believe that our estimates of yield losses under a future scenario may be conservative. Current and increased concentrations of ground level ozone have been shown to lead to decreases in plant biomass and yield (Morgan et al., 2003; Gitay et al., 2001). Independently of climate change, but exacerbated by it, surface ozone concentrations are expected to increase globally. Thus, if the effects of ozone are to be included in an assessment of crop yields in the Mediterranean under a future climate scenario, the results are likely to be greater yield reductions than presented here.

As expected, the northern Mediterranean region is likely to reduce energy use in the winter due to reduced heating demands. However, during summer, substantial

increases in energy demand are expected everywhere and especially in the south. The peak in energy demand hence falls in the dry season, which is expected to become even drier in the future. A low water supply reduces energy production from hydroelectric plants, as well as from conventional power plants which require water for cooling and for driving the turbines. As a result, energy demands may not be able to be met in the warm period of the year. Additional capacity may need to be installed unless adaptation or mitigation strategies are to put into place. On the other hand, conditions for renewable energy production, such as solar and wind energy, may improve under climate change. For instance, data from Spain show that the response of mean daily demand for electricity to an increase of 1°C has steadily increased over the past 30 years (Rodriguez et al., 2005). The energy demand for cooling is likely to continue to rise as a society becomes richer and increased incomes allow the population to afford more comfort. More air conditioning facilities could be installed. In turn, the heat generated by air conditioning units could raise temperatures further and further increase the demand for cooling. Conditions for tourism are expected to improve in northern and western Europe. Mediterranean countries will probably experience a lengthening and a flattening of their tourism season by 2030. Higher summer temperatures may lead to a gradual decrease in summer tourism in the Mediterranean but an increase in spring and autumn.

Acknowledgments

This work was supported by WWF International and by the European Commission ENSEMBLES project (Contract number GOCE-CT-2003-505539, www.ensembles-eu.org).

References

Ainsworth EA, Long SP, 2005. What have we learned from 15 years of free-air CO_2 enrichment (FACE)? A meta-analytic review of responses to rising CO_2 in photosynthesis, canopy properties and plant production. *New Phytol*., 165:351-372

Beniston, M., 2004. The 2003 heatwave in Europe: A shape of things to come? An analysis based on Swiss climatological data and model simulations, *Geophys. Res. Let.*, 31, doi:10.1029/2003GL018857

Bolle H-J (ed) (2003) Mediterranean climate. Variability and trends. Springer, Berlin Heildelburg New York

Christensen J. H., Carter T. R., Giorgi F., 2002. PRUDENCE employs new methods to assess European climate change, *EOS* 83:147

Christensen J.H. and O.B.Christensen, 2007. A summary of the PRUDENCE model projections of changes in European climate by the end of this century. Climatic Change, 81, 7-30.

Déqué, M., P. Marquet, and R.G. Jones, 1998. Simulation of climate change over Europe using a global variable resolution general circulation model, Clim. Dyn., vol. 14, pp. 173-189.

Déqué, M., D. P. Rowell, D. Lüthi, F. Giorgi, J. H. Christensen, B. Rockel, D. Jacob, E. Kjellström, M. de Castro and B. van den Hurk , 2007. An intercomparison of regional climate simulations for Europe: assessing uncertainties in model projections. Climatic Change, 81, 53-70.

Giannakopoulos C. and B.Psiloglou, Trends in energy load demand for Athens, Greece: weather and non-weather related factors, Climate Research, 13, 97-108, 2006.

Gibelin, A.-L. and M. Déqué, 2002. Anthropogenic climate change over the Mediterranean region simulated by a global variable resolution model, Clim. Dyn., Volume 20, Issue 4, pp. 327-339

Giorgi, F.; Marinucci, M. R.; Visconti, G., 1992. A $2XCO_2$ climate change scenario over Europe generated using a limited area model nested in a general circulation model 2. Climate change scenario, *J. Geophys. Res*., 97, D9, 10011-10028, doi:10.1029/92JD00614.

Giorgi, F., X. Xunqiang, J. Pal., 2004. Mean, interannual variability and trends in a regional climate change experiment over Europe. II: climate change scenarios (2071-2100), *Clim. Dyn.*, 23: 839-858, doi: 10.1007/s00382-004-0467-0

Gitay H, Brown S, Easterling W and Jallow B. (2001) Ecosystems and their goods and services, In: *Climate Change 2001: Impacts, Adaptation and Vulnerability*, McCarthy, JJ Canziani, OF, Leary, NA, Dokken DJ and White KS (ed.), p.735-800.

Good P, M. Moriondo, C. Giannakopoulos and M. Bindi, 2008. The meteorological conditions associated with extreme fire risk in Italy and Greece: relevance to climate model studies. *International Journal of Wildland Fire* 17(2) 155–165

Gordon, C., C. Cooper, C.A. Senior, H. Banks, J.M. Gregory, T.C. Johns, J.F.B. Mitchell and R.A. Wood, 2000. The simulation of SST, sea ice extents and ocean heat transports in a version of the Hadley Centre coupled model without flux adjustments, *Clim. Dyn.*, 16: 147-168.

Hanson, C.E., J.P. Palutikof, M.T.J. Livermore, L. Barring, M. Bindi, J. Corte-Real, R. Duaro, C. Giannakopoulos, T. Holt, Z. Kundzewicz, G. Leckebusch, M. Radziejewski, J. Santos, P. Schlyter, M. Schwarb, I. Stjernquist, U. Ulbrich, Modeling the Impact of Climate Extremes: An overview of the MICE Project, Climatic Change, PRUDENCE Special Issue, 81, 163-177, 2007.

IPCC, 2001a. Climate Change 2001: Impacts, Adaptation and Vulnerability. Contribution of Working Group II to the Third Assessment Report of the Intergovernmental Panel on Climate Change. Cambridge University Press.

IPCC, 2001b. Climate Change 2001: The Scientific Basis. Contribution of Working Group I to the Third Assessment Report of the Intergovernmental Panel on Climate Change [Houghton, J.T., Y. Ding, D.J. Griggs, M. Noguer, P.J. van der Linden, X. Dai, K. Maskell, and C.A. Johnson (eds.)]. Cambridge University Press, Cambridge, United Kingdom and New York, NY, USA, 881pp.

IPCC, 2007. Climate Change 2007: The Physical Science Basis. Contribution of Working Group I to the Fourth Assessment Report of the Intergovernmental Panel on Climate Change [Solomon, S., D. Qin, M. Manning (eds.)].

Jones, R. G., Murphy, J. M., Noguer, M., Keen, A. B., 1997. Simulation of climate change over Europe using a nested regional-climate model. II: Comparison of driving and regional model responses to a doubling of carbon dioxide, *Quarterly Journal of the Royal Meteorological Society*, vol. 123, Issue 538, p.265-292

Kimball BA, Kobayashi K, Bindi M (2002) Responses of agricultural crops to free-air CO_2 enrichment. *Advances in Agronomy*, 77: 293-368

Kostopoulou, E. and P. D. Jones, 2005. Assessment of climate extremes in the eastern Mediterranean, *Meteor. Atmos. Phys.*, 89, 69-85.

Lionello P., P. Malanotte and R. Boscolo, (Eds), 2006. Mediterranean Climate Variability, Elsevier B.V., Amsterdam.

Morgan PB, Ainsworth EA, Long SP (2003) How does elevated ozone impact soybean? A meta-analysis of photosynthesis, growth and yield. *Plant, Cell and Environment* 2003 26:8 1317

Moriondo, M, P. Good, R. Durao, M. Bindi, C. Giannakopoulos and J. Corte-Real, 2006. Potential impact of climate change on fire risk in the Mediterranean area. Climate Research vol. 31, Issue 1, 85-95.

Mudelsee M. and Alkio M., 2007. Quantifying effects in two-sample environmental experiments using bootstrap confidence intervals. Environmental Modelling & Software 22:84–96.

Nakicenovic N, Alcamo J, Davis G, de Vries B, Fenhann J, Gaffin S, Gregory K, Grübler A, Jung TY, Kram T, La Rovere EL, Michaelis L, Mori S, Morita T, Pepper W, Pitcher H, Price L, Raihi K, Roehrl A, Rogner HH, Sankovski A, Schlesinger M, Shukla P, Smith S, Swart R, van Rooijen S, Victor N and Dadid Z. 2000. Emissions scenarios. A Special Report of Working Group III of the Intergovernmental Panel on Climate Change. Cambridge University Press, Cambridge, U.K., 599 pp. Available online at: http://www.grida.no/climate/ipcc/emission/index.htm.

New, M., 2005. Arctic climate change with a 2°C global warming. In Rosentrater L (Ed.): Evidence and Implications of Dangerous Climate Change in the Arctic, *WWF International Arctic Program*.

Perry, A., 2001: More heat and drought - Can Mediterranean tourism survive and prosper?, In Proceedings of the First International Workshop on Climate, Tourism and Recreation, A. Matzarakis and C.R. De Freitas, eds., 1-6, International Society of Biometeorology.

Perry A. 2005. The Mediterranean: How can the world's most popular and successful tourist destination adapt to a changing climate. In: Tourism, Recreation, And Climate Change (Aspects of Tourism). C. Michael Hall (Editor), James E. S. Higham (Editor)

Pope, V. D., M. L. Gallani, P. R. Rowntree and R. A. Stratton, 2000. The impact of new physical parameterizations in the Hadley Centre climate model -- HadAM3, *Clim. Dyn.*, 16: 123-146.

Räisänen, J., U. Hansson, A. Ullerstig, R. Döscher, L. P. Graham, C. Jones, H. E. M. Meier, P. Samuelsson, and U. Willén, 2003. European climate in the late twenty-first century: regional simulations with two driving global models and two forcing scenarios, *Clim. Dyn.*, 22: 13-31.

Romero, R., C. Ramis, and J. A. Guijarro, 1999. Daily rainfall patterns in the Spanish Mediterranean area: an objective classification, *Inter. J. of Clim.,* 19, 95-112.

Schär C, Vidale P, Lüthi D, Frei C, Häberli C, Liniger MA, Appenzeller C, 2004 The role of increasing temperature variability for European summer heatwaves Nature, 427, 332-336

Stockle CO, Donatelli M, Nelson R (2003) CropSyst, a cropping systems simulation model. *Eur J Agron* 18: 289-307

Türkeş, M., U. M. Sumer, and G. Kilic, 2002. Persistence and periodicity in the precipitation series of Turkey and associations with 500 hPa geopotential heights, *Climate Research,* 21, 59-81.

WTO (2004a) World Tourism Barometer, WTO, vol. 2, no. 1, January 2004, p 23

WTO (2004b) World Tourism Barometer, WTO, vol. 2, no. 2, June 2004, p 22

Xoplaki, E., J. Luterbacher, R. Burkard, I. Patrikas, and P. Maheras, 2000. Connection between the large scale 500 hPa geopotential height fields and precipitation over Greece during wintertime, *Climate Research,* 14, 129-146.

Table 1: Type of crop simulated in each of the selected grid cell

Grid cell number	Country	C4 summer crop	C3 summer crop	Legumes	Tuber crops	Cereals
1	Portugal	maize	sunflower	bean	potato	wheat
2	Spain	maize	sunflower	lentil	potato	barley
3	France	maize	sunflower	soybean	potato	wheat
4	Italy	maize	sunflower	soybean	potato	wheat
5	Serbia	maize	sunflower	soybean	potato	wheat
6	Greece	maize	sunflower	bean	potato	wheat
7	Turkey	maize	sunflower	lentil	potato	wheat
8	Jordan	maize	sunflower	lentil	potato	barley
9	Egypt	maize	sunflower	bean	potato	wheat
10	Libya	maize	sunflower	bean	potato	wheat
11	Tunisia	maize	sunflower	bean	potato	wheat
12	Algeria	maize	sunflower	bean	potato	wheat
13	Morocco	maize	sunflower	bean	potato	wheat

Table 2: Mean Absolute Error (MAE, %) between observed and simulated crop yields for the main Mediterranean regions: N-W = Portugal, Spain, France and Italy, N-E = Serbia, Greece and Turkey, S-E = Jordan, Egypt and Libya, S-W = Tunisia, Algeria and Morocco

	Mean Absolute Error (MAE, %)				
Region	**C4 summer**	**Legumes**	**C3 summer**	**Tuber crops**	**Cereals**
N-W	9.3	4.6	10.8	8.7	9.8
N-E	4.4	1.4	2.1	6.7	4.3
S-E	12.1	13.8	4.4	11.7	1.3
S-W	13.4	0.9	2.7	3.3	6.4

Table 3: Summary of climate changes and their probable impact on major travel flows in the Mediterranean.

Major Tourism Flow	Origin Market Climate Change	Destination Region Climate Change	Implications for Destination Region	Possible Market Reactions
Northern Europe to Mediterranean	• Warmer, wetter winters • Warmer, drier summers • More reliable summers	• Warmer winters • Warmer, drier summers • Increased heat index • Frequent heatwaves • More arid landscape • Small tidal range (i.e. greater sea level rise impact)	• Greater drought and fire risk • Increased water shortages • Greater human heat stress • Beach degradation and habitat loss (due to sea level rise) • Vulnerability to tropical diseases (e.g. malaria) • Frequent flash floods • Poor urban air quality in cities	• Improvement of Northern European summers triggers more domestic holidays • Decreased incentive for Mediterranean summer holidays • Increased incentive for shoulder month Mediterranean holidays • Increased incentive for southerners to go north

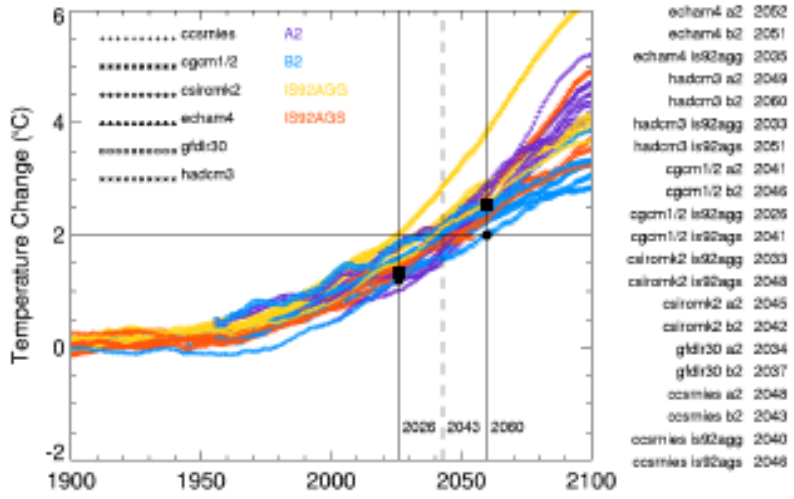

Fig. 1. Global mean annual temperature anomalies relative to control climatology, smoothed with a 21-year moving average. Vertical lines indicate the range in time at which the 21-year global mean temperature anomaly exceeds +2°C. The two black circles (squares) indicate the HadCM3-A2 (B2) temperature at this range limits. Numbers on the right show the time at which the 21-year mean global temperature anomaly exceeds +2°C for each GCM-scenario combination. (Adapted from *New* (2005)).

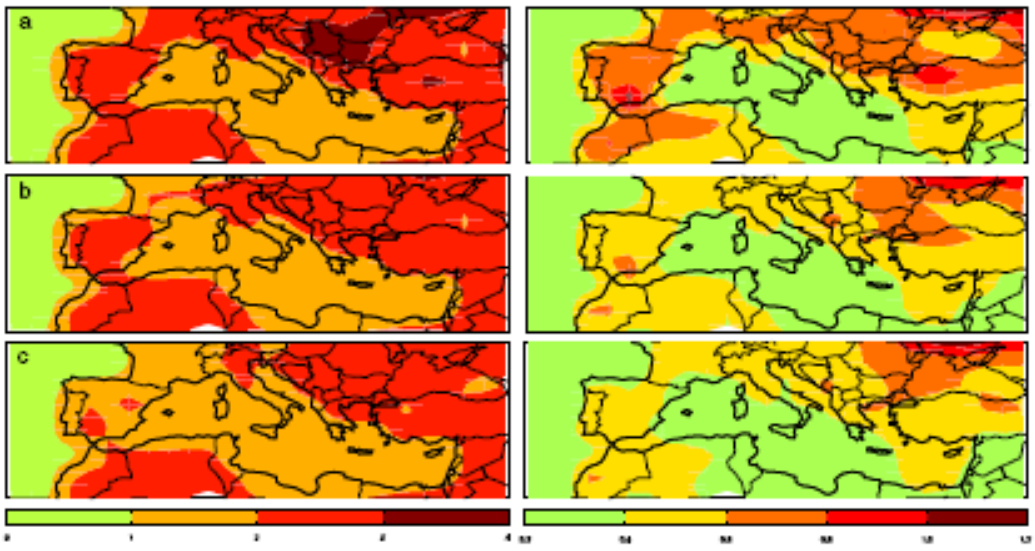

Fig. 2. Left column: difference between the daily (a) maximum, (b) mean, and (c) minimum temperature (°C) averaged over 2031-2060 and over 1961-1990. Right column: the corresponding 95% confidence range.

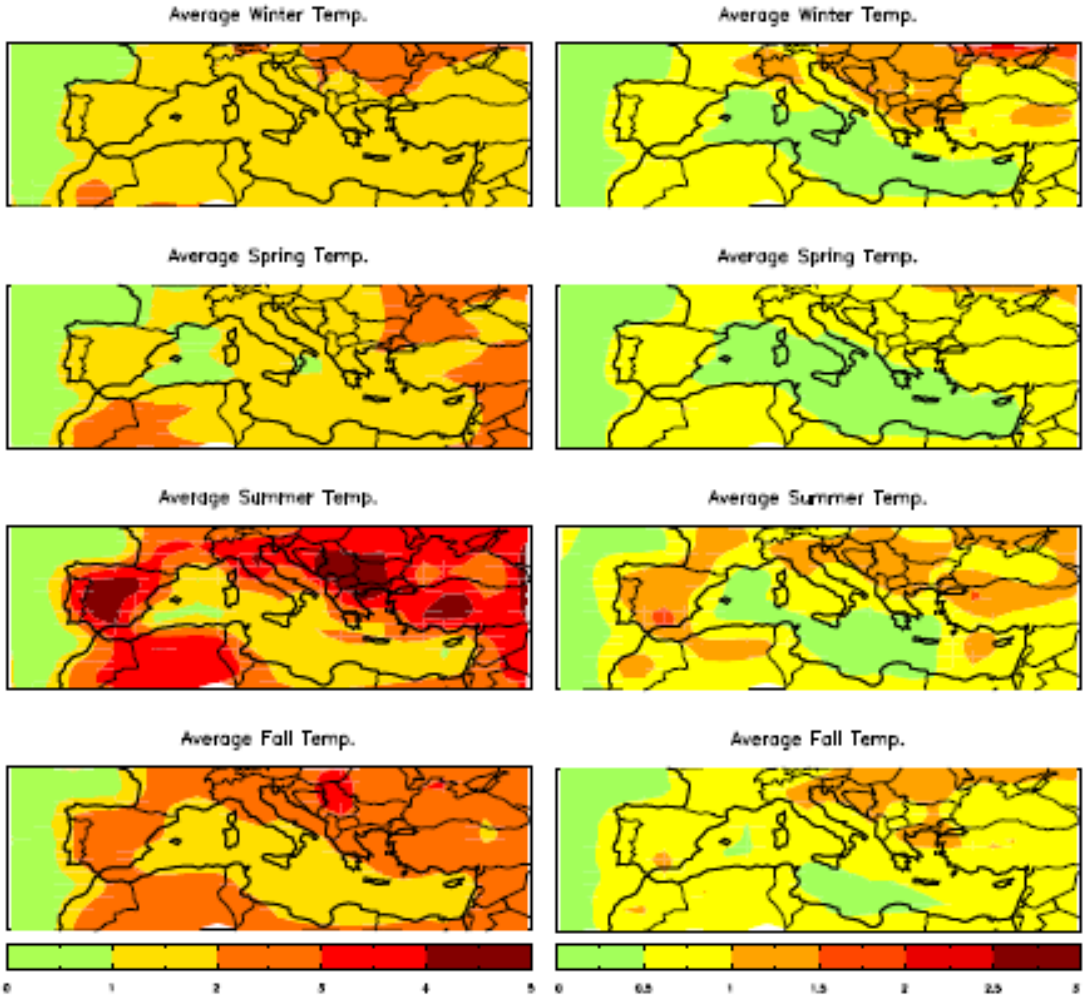

Fig. 3. Difference between the daily mean temperatures averaged over (a) winter, (b) spring, (c) summer, and (d) autumn months of 2031-2060 and 1961-1990.

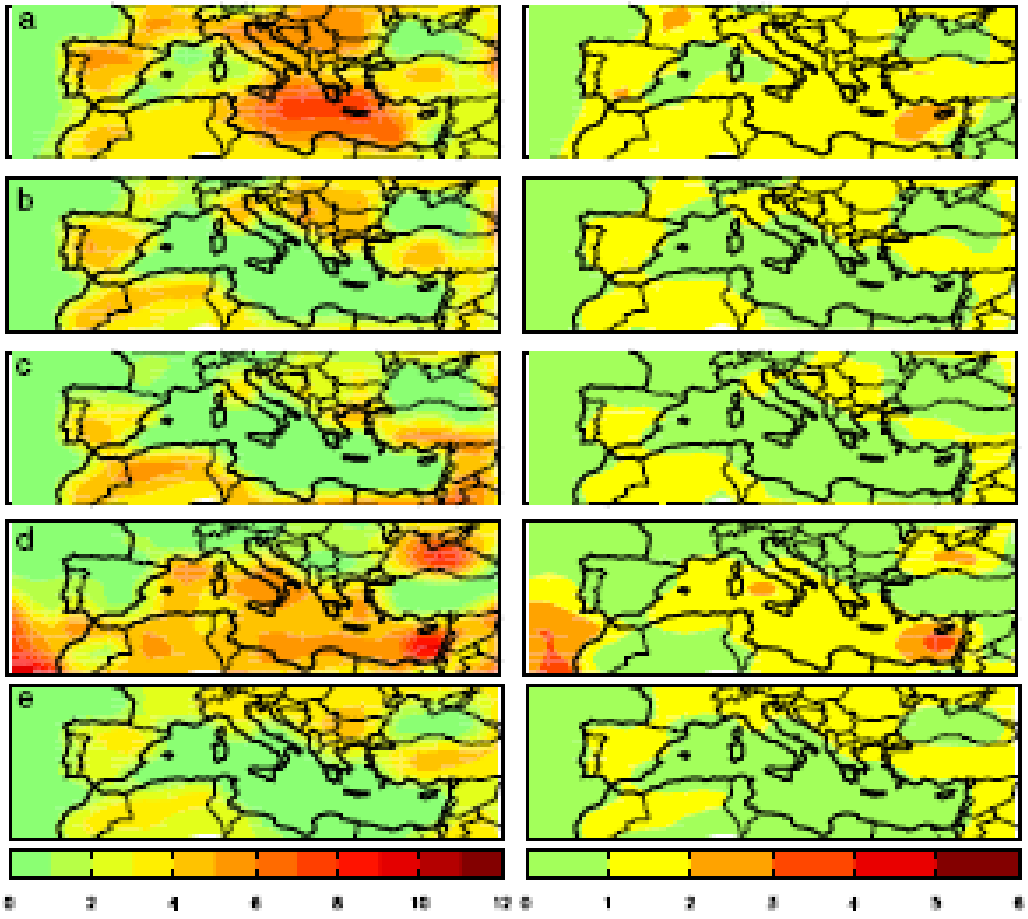

Fig. 4. Left column: increase in the number of (a) summer days, (b) hot days, (c) heatwave days, and (d) tropical nights, and (e) decrease in the number of frost nights between 1961-1990 and 2031-2060. Averaged annual numbers are considered and units are weeks. Right column: the corresponding 95% confidence range in week.

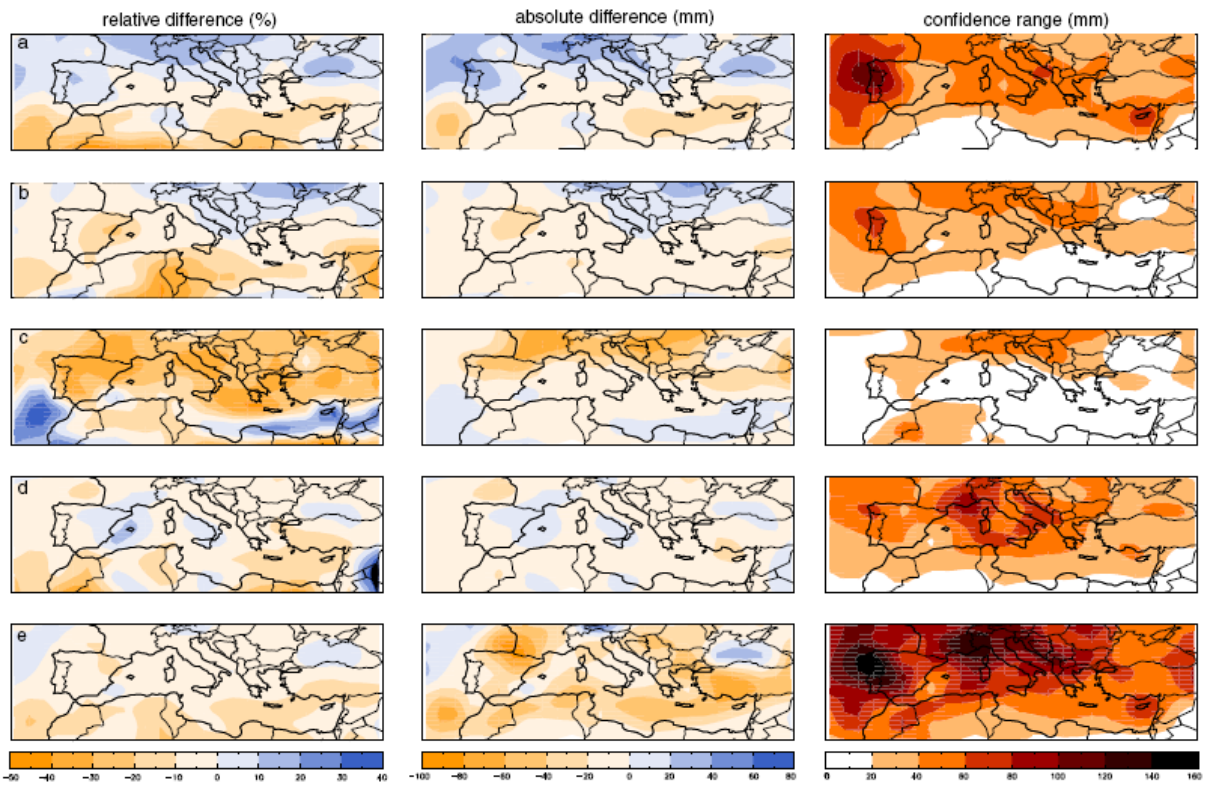

Fig. 5. Centre column: average changes in annual rainfall accumulated over (a) winter, (b) spring, (c) summer, (d) autumn, and (e) the full year between 2031-2060 and 1961-1990. Units are mm. Right column: corresponding 95% confidence range in mm. Left column: changes in percentage of 1961-1990 average values.

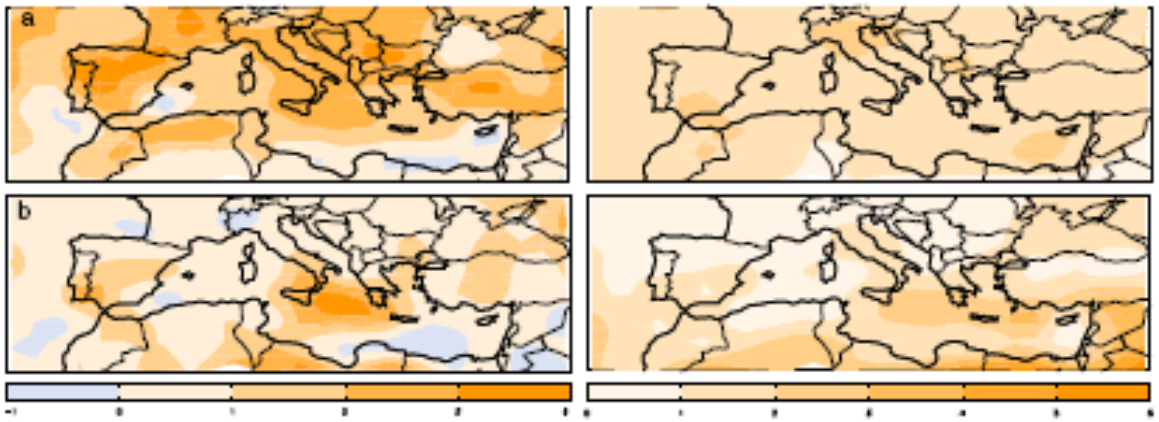

Fig. 6. Left column: Differences in annual (a) number of dry days and (b) length of longest dry spell averaged over 2031-2060 and over 1961-1990, in week units. Right column: corresponding 95% confidence range in weeks.

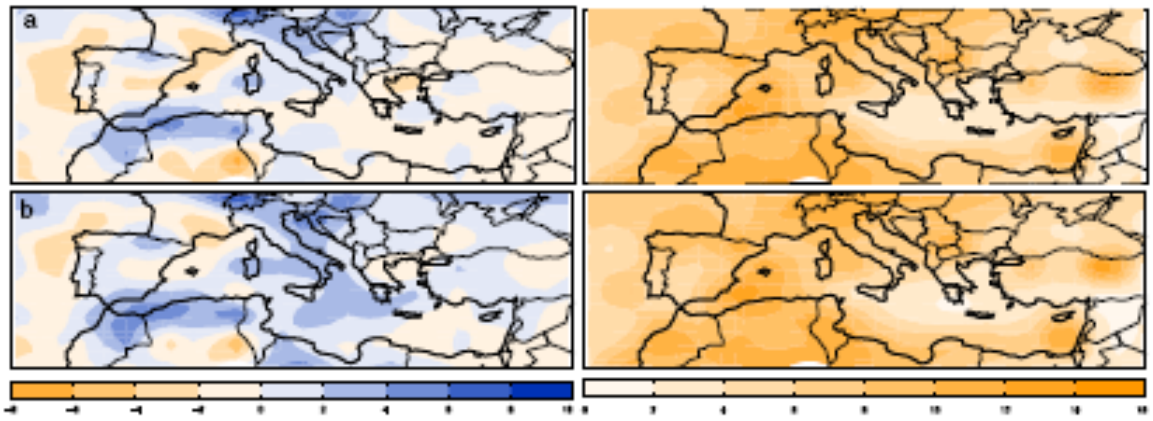

Fig. 7. Averaged shift of (a) start and (b) end of the longest dry spell between 2031-2060 and 1961-1990, in weeks. Right: corresponding 95% confidence range.

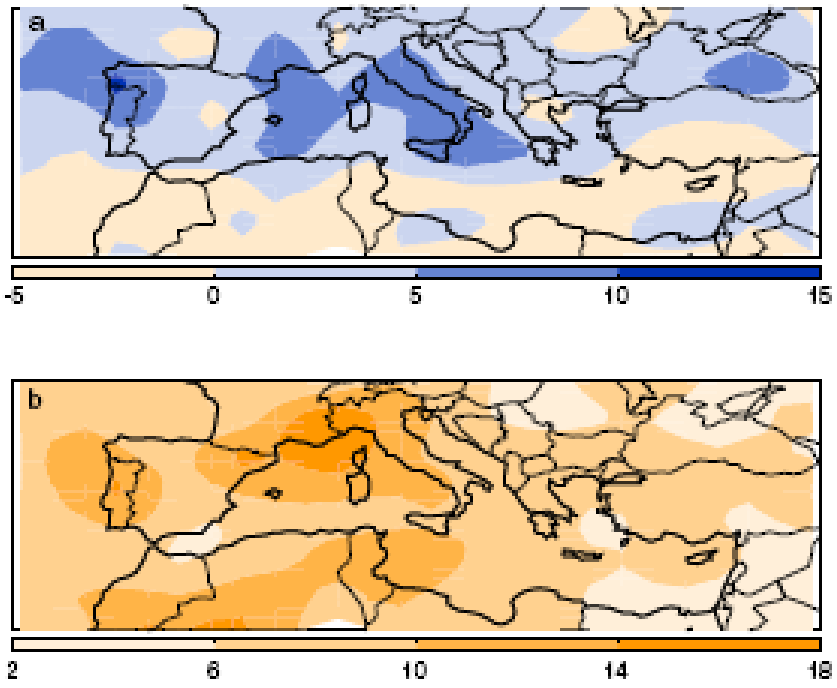

Fig. 8. Top: averaged difference in annual maximum running total rainfall over three days between 2031-2060 and 1961-1990 in mm. Bottom: corresponding 95% confidence range.

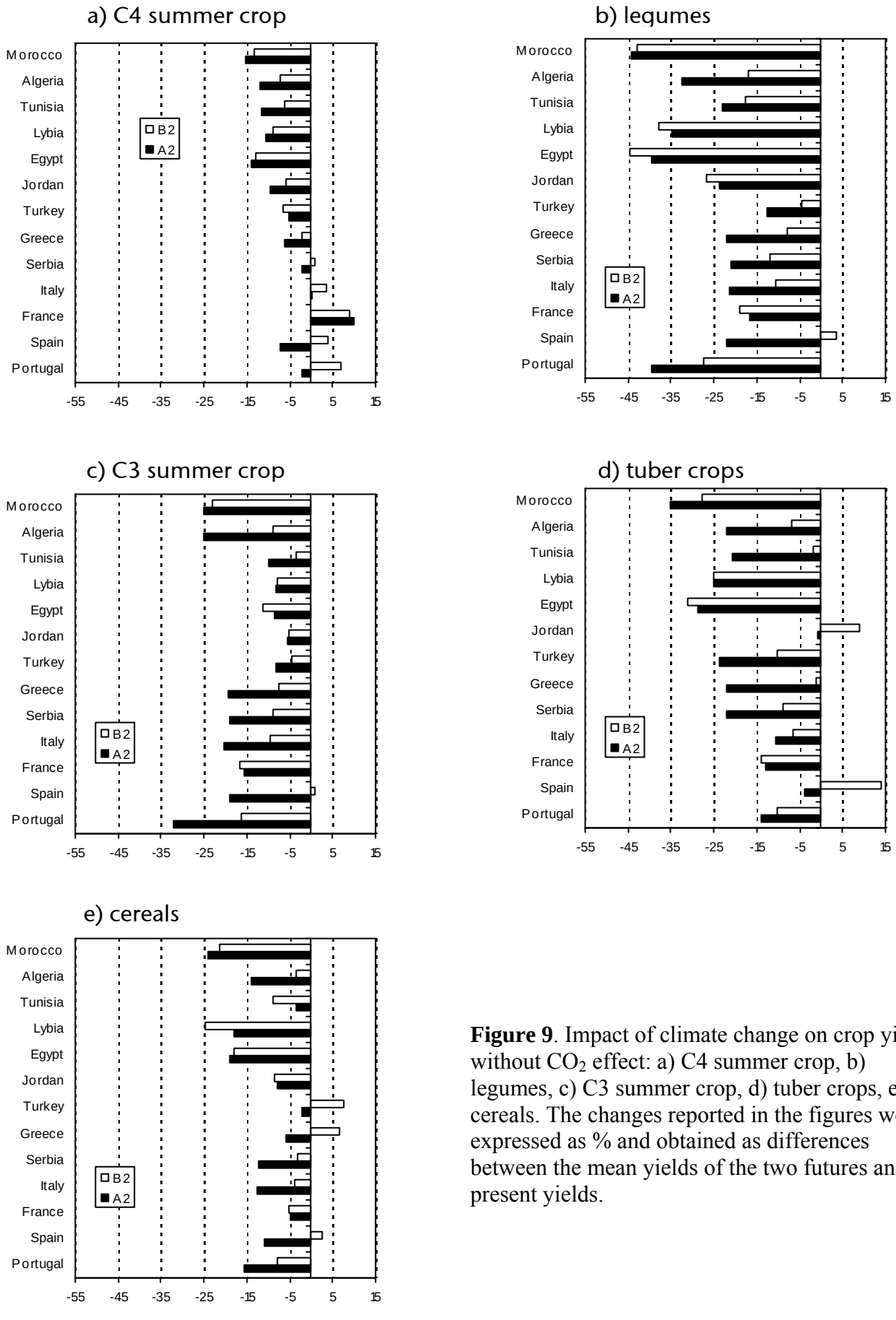

Figure 9. Impact of climate change on crop yields without CO_2 effect: a) C4 summer crop, b) legumes, c) C3 summer crop, d) tuber crops, e) cereals. The changes reported in the figures were expressed as % and obtained as differences between the mean yields of the two futures and the present yields.

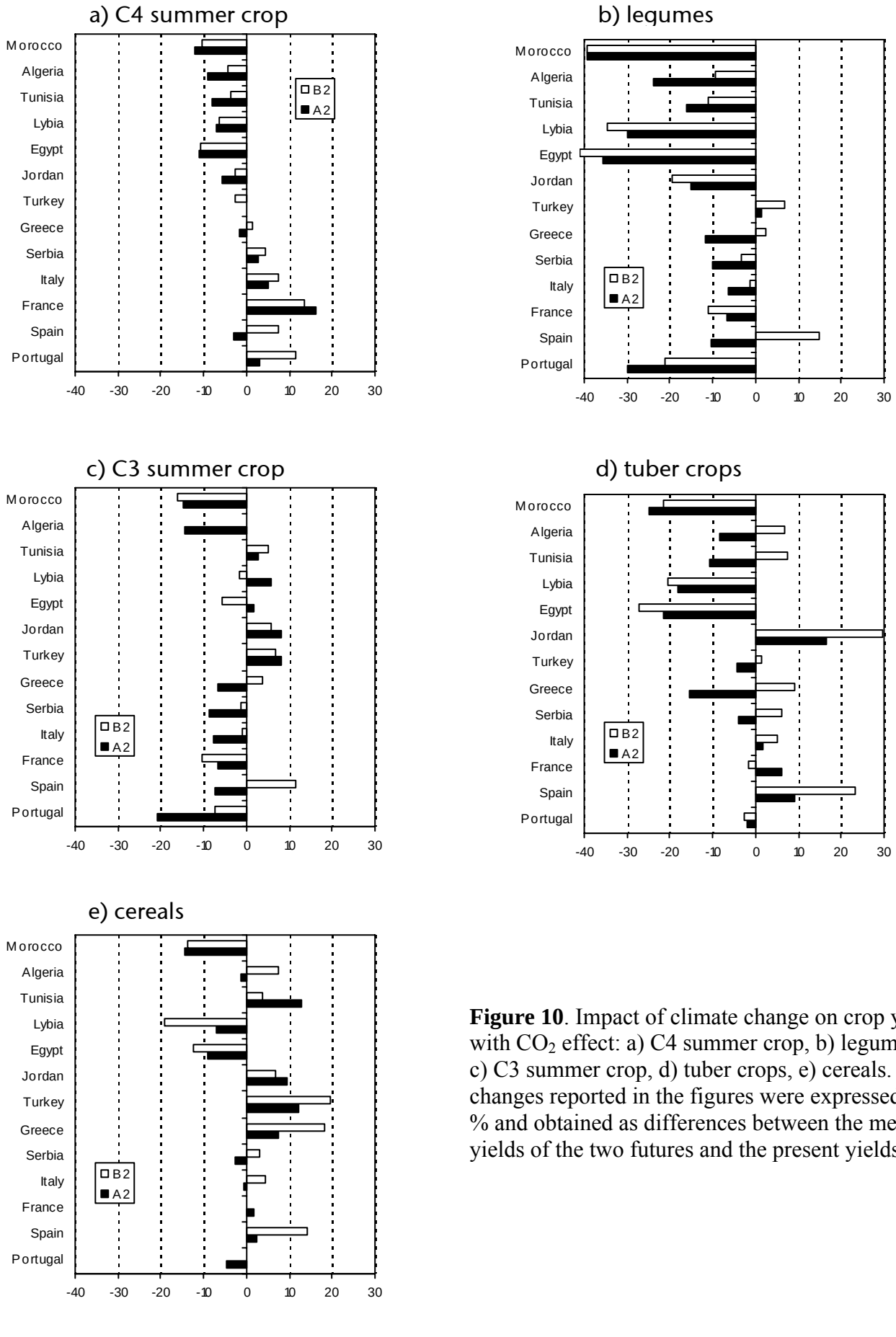

Figure 10. Impact of climate change on crop yields with CO_2 effect: a) C4 summer crop, b) legumes, c) C3 summer crop, d) tuber crops, e) cereals. The changes reported in the figures were expressed as % and obtained as differences between the mean yields of the two futures and the present yields.

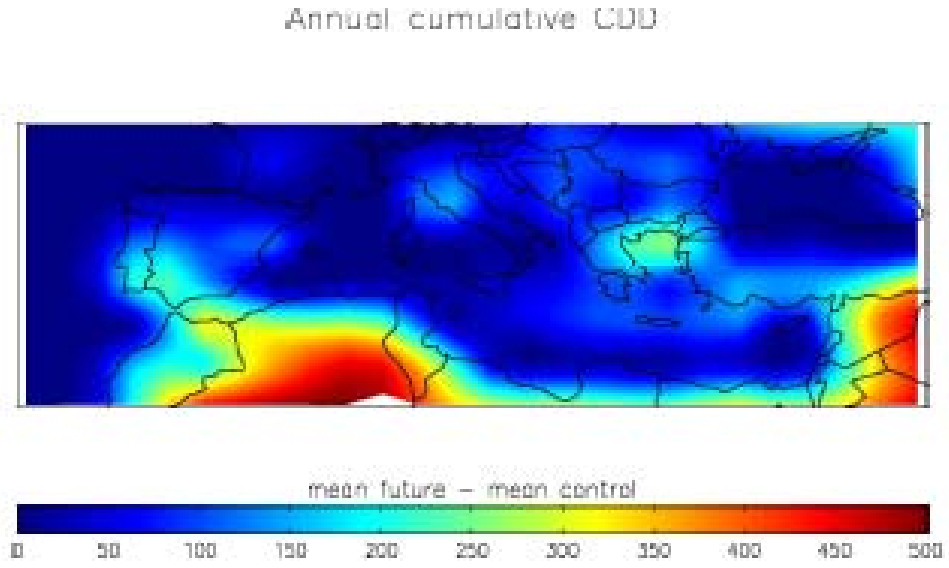

Fig. 11. Changes in average yearly cumulative CDD between the future and control period.

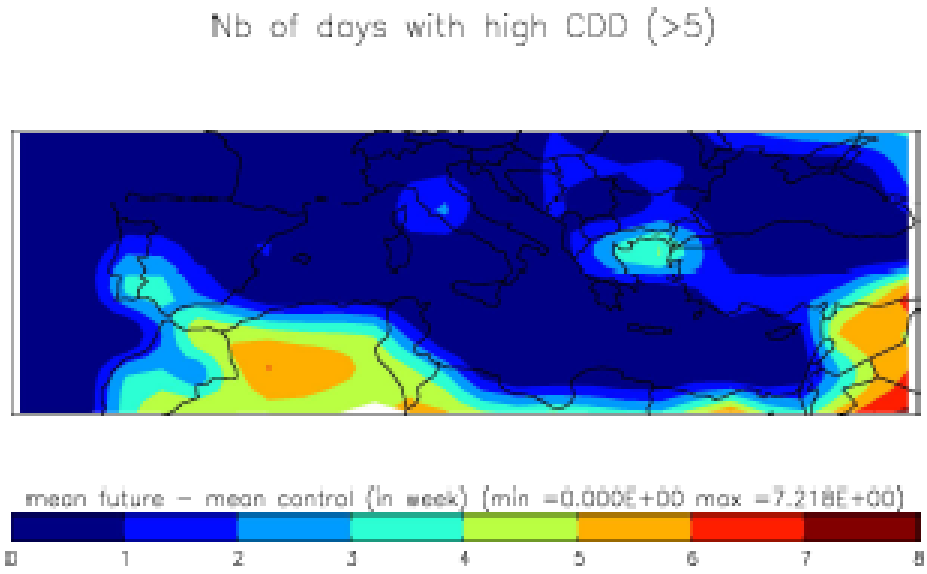

Fig. 12. Changes in the number of days with large cooling demand (CDD >5) between the future and control period.

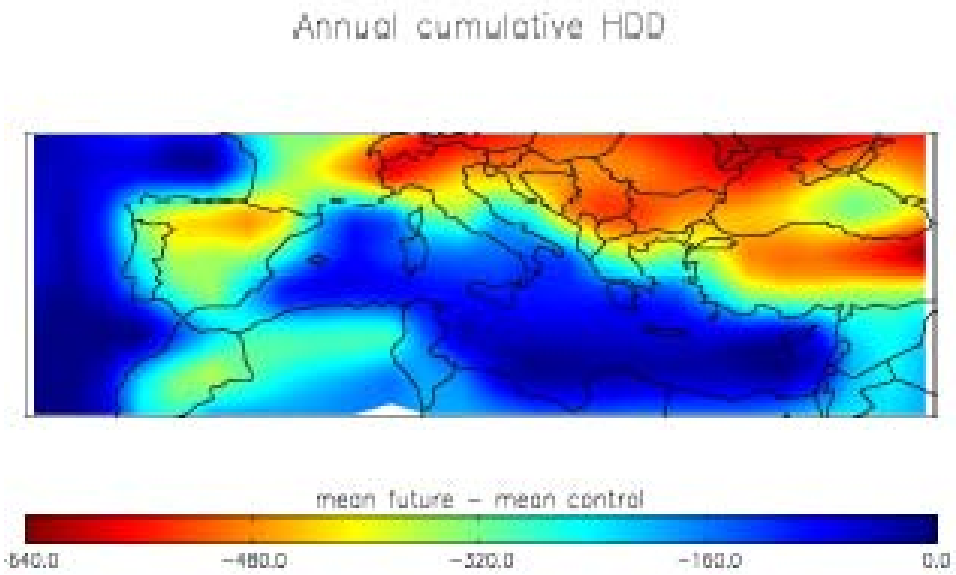

Fig. 13. Changes in average yearly cumulative HDDs between the future and control period.

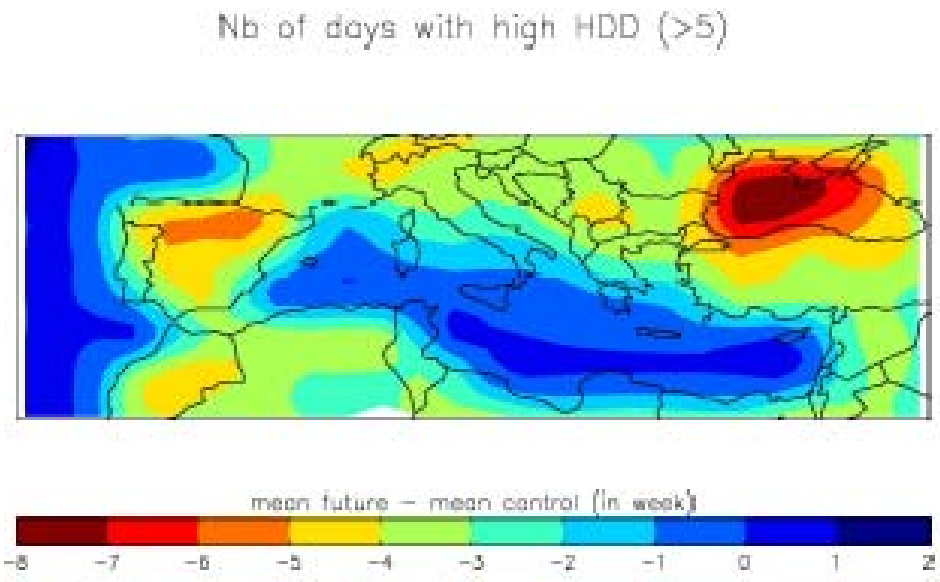

Fig. 14. Changes in the number of days with large heating demand (HDD >5) between the future and control period.

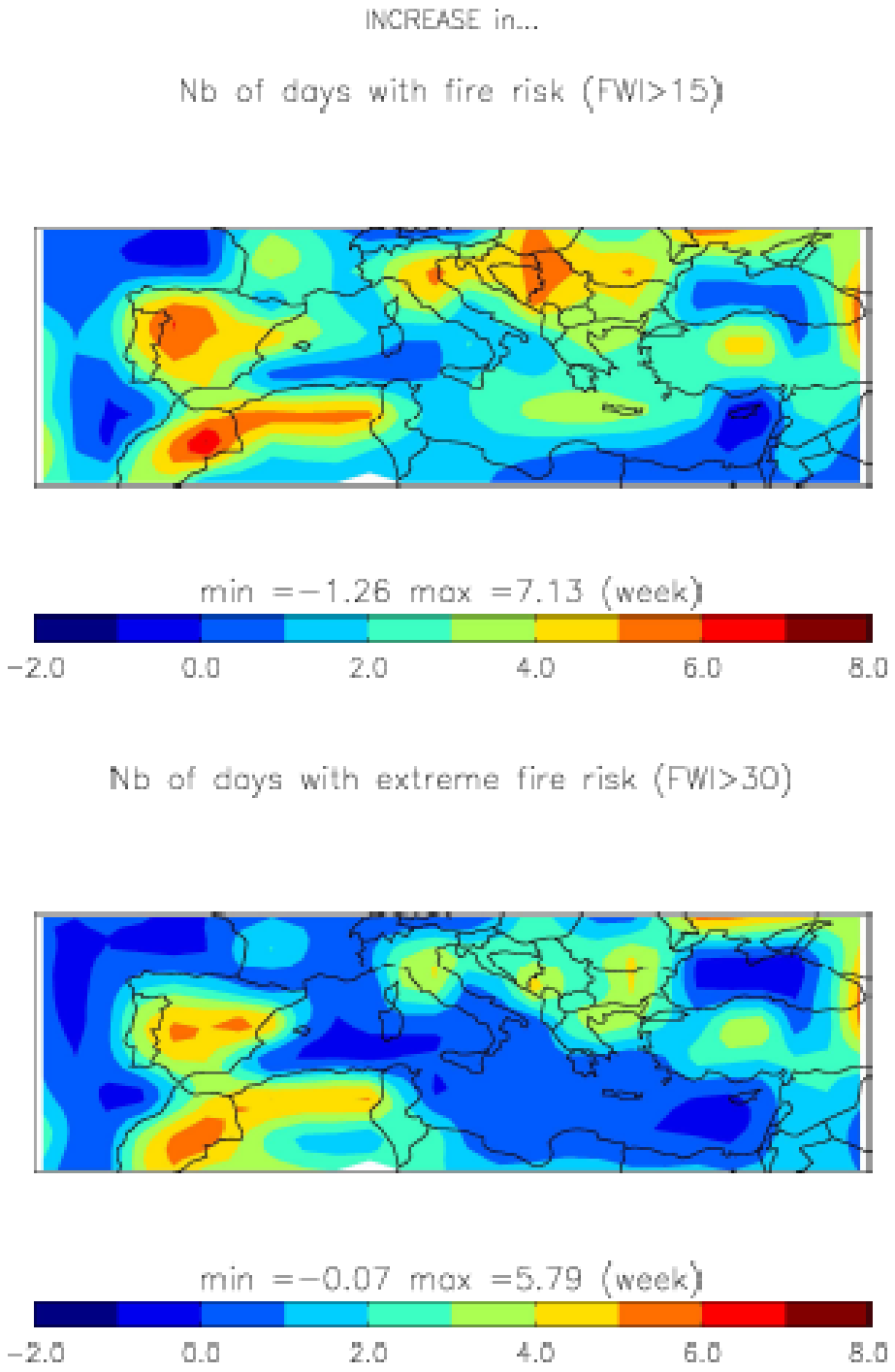

Fig. 15. Changes in the number of weeks with fire risk (top) and extreme fire risk (bottom) between the future and the control period.